JACS
JOURNAL OF THE AMERICAN CHEMICAL SOCIETY

COMMUNICATION

pubs.acs.org/JACS

# Insight into the Cation−$\pi$ Interaction at the Metal Binding Site of the Copper Metallochaperone CusF

Dhruva K. Chakravorty, Bing Wang, Melek N. Ucisik, and Kenneth M. Merz, Jr.*

Department of Chemistry and Quantum Theory Project, University of Florida, 2238 New Physics Building, P.O. Box 118435, Gainesville, Florida 32611-8435, United States

Supporting Information

**ABSTRACT:** The periplasmic $Cu^+/Ag^+$ chaperone CusF features a novel cation−$\pi$ interaction between a $Cu^+/Ag^+$ ion and Trp44 at the metal binding site. The nature and strength of the $Cu^+/Ag^+$−Trp44 interactions were investigated using computational methodologies. Quantum-mechanical (QM) calculations showed that the $Cu^+$ and $Ag^+$ interactions with Trp44 are of similar strength (∼14 kcal/mol) and bond order. Quantum-mechanical/molecular-mechanical (QM/MM) calculations showed that $Cu^+$ binds in a distorted tetrahedral coordination environment in the Trp44Met mutant, which lacks the cation−$\pi$ interaction. Molecular dynamics (MD) simulations of CusF in the apo and $Cu^+$-bound states emphasized the importance of the $Cu^+$−Trp44 interaction in protecting $Cu^+$ from water oxidation. The protein structure does not change over the time scale of hundreds of nanoseconds in the metal-bound state. The metal recognition site exhibits small motions in the apo state but remains largely preorganized toward metal binding. Trp44 remains oriented to form the cation−$\pi$ interaction in the apo state and faces an energetic penalty to move away from the metal ion. $Cu^+$ binding quenches the protein's internal motions in regions linked to binding CusB, suggesting that protein motions play an essential role in $Cu^+$ transfer to CusB.

Heavy-metal homeostasis regulates the concentration of metal ions in cells and is essential for the survival of organisms.[1] A strong coupling between heavy-metal tolerance and antibiotic resistance in Gram-negative bacteria makes it imperative to understand the nature of $Cu^+/Ag^+$ efflux in these organisms. In *Escherichia coli*, the *cus* determinant consisting of the *cusCFBA* operon provides for $Cu^+$ and $Ag^+$ resistance.[2,3] Recent crystal structures have suggested that the CusCBA proteins combine to form a tripartite cation efflux pump that expels metal ions from within the cell to the outer membrane.[4] CusF is a small $\beta$-barrel protein [Figure 1 and Figure SI.1 in the Supporting Information (SI)] that functions as a periplasmic $Cu^+/Ag^+$ metallochaperone.[5] It binds to CusB and provides $Cu^+/Ag^+$ efflux directly from the periplasm by transferring metal ions to the tripartite cation efflux pump.[3] CusF is not essential for $Cu^+/Ag^+$ ion tolerance, and its exact role in heavy-metal homeostasis remains a subject for further investigation.[6]

The crystallographic structures of the apo and holo forms of CusF are similar, indicating that metal ion binding does not cause a large change in the protein structure.[5,7,8] The metal recognition site in CusF is located in a hydrophobic environment and contains a novel cation−$\pi$ interaction between $Cu^+/Ag^+$ and the Cε3 and Cζ3 carbon atoms on the aromatic ring of the neighboring Trp44 residue (Figure 1 and Figures SI.1−SI.3). In addition to this interaction, His36, Met47, and Met49 residues bind to the $Cu^+/Ag^+$ ion in a distorted trigonal-planar arrangement in which the metal ion is slightly elevated from the plane (Figure 1). An exact characterization of the unique $Cu^+/Ag^+$−W44 interaction has been hampered by a lack of direct spectroscopic evidence. A crystallographic database search of similar compounds by Xue et al.[7] found this interaction to lie at the periphery of nonbonded interactions, while UV resonance Raman spectroscopy identified this interaction as a novel cation−$\pi$ interaction rarely observed in a $Cu^+/Ag^+$ metal binding site. Experiments by Loftin et al.[9] have suggested that Trp44 protects $Cu^+/Ag^+$ from oxidative stress in the periplasm. The role of the cation−$\pi$ interaction in the function of CusF remains unclear, as a W44M mutation exists in 25% of CusF proteins. The W44M mutant of CusF is known to have a higher binding affinity for $Cu^+$.[7,9] While the nature of the metal coordination in the metal binding site of the W44M mutant (which lacks the cation−$\pi$ interaction) has been probed with extended X-ray absorption fine structure (EXAFS), the exact geometry of the metal binding site remains to be determined.[9]

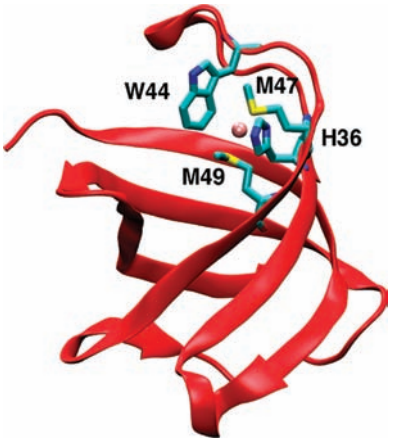


**Figure 1.** Cartoon representation of Cu(I)·CusF (PDB entry 2VB2). $Cu^+$ is shown as a pink sphere, and the metal binding residues are represented as sticks.

**Received:** September 22, 2011
**Published:** October 26, 2011

 © 2011 American Chemical Society 

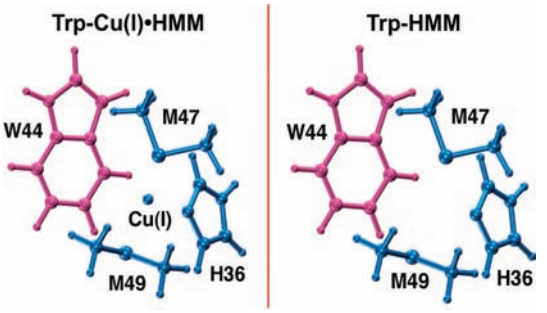


**Figure 2.** $Cu^+$·CusF metal-binding-site geometries represented using a model system. Interaction energies between the pink and blue fragments were calculated. The Trp−Cu(I)·HMM interaction energy is the energy of the interaction between W44 and bound $Cu^+$ (W44−$Cu^+$·H36·M47·M49), and the Trp−HMM interaction energy is the energy of the interactions between W44 and other metal binding residues in the absence of $Cu^+$ (W44−H36·M47·M49) at the same geometry. The stabilization from the cation−$\pi$ interaction was estimated as Trp−Cu(I)·HMM − Trp−HMM.

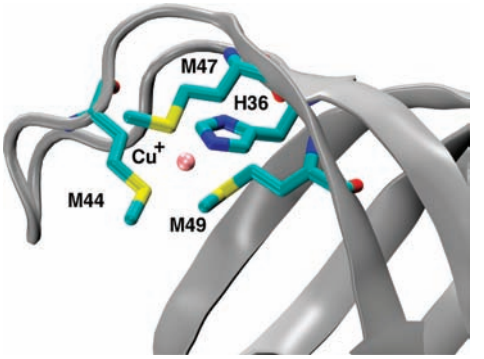


**Figure 3.** Cartoon representation of the Cu(I)·W44M CusF mutant obtained from QM/MM calculations. $Cu^+$ is shown as a pink sphere, and the metal binding residues that form a distorted tetrahedral coordination environment are represented as sticks.

In this study, we investigated the nature of the $Cu^+/Ag^+$−W44 interaction and evaluated its impact on the chaperone function of CusF using computational methodologies. We have estimated the strength of this interaction and provided a quantum-mechanical (QM) basis for its characterization using accurate ab initio calculations. We used quantum-mechanical/molecular-mechanical (QM/MM) calculations to evaluate the role of W44 in protecting $Cu^+$ and propose a metal binding geometry for $Cu^+$ in the W44M mutant. In addition, we performed molecular dynamics (MD) simulations to investigate changes in the structure and internal motions of the protein related to $Cu^+$ binding. These simulations provide deeper insight into the role of the cation−$\pi$ interaction and its relation to the protein's function. In this study, all ab initio calculations were performed using the Gaussian 09 suite of programs,[10] QM/MM calculations were performed using the Qsite in the Schrödinger suite of programs,[11] and MD simulations were performed using the Amber 11 suite of programs.[12] MD trajectories were analyzed using the VMD suite of programs[13] and the ptraj utility in AmberTools 1.5. The first nine residues of CusF were not included in the analysis of MD trajectories. Complete details for all calculations are included in Methods and Results in the SI.

We performed QM calculations at the second-order Møller−Plesset perturbation theory (MP2) level to determine the strength of the $Cu^+/Ag^+$−W44 cation−$\pi$ interaction in the $Cu^+$- and $Ag^+$-bound crystal structure geometries of the protein (Figure 2). A double-$\zeta$-quality LANL2DZ pseudopotential-based basis set[14] was used for $Ag^+$, while the augmented Dunning correlation-consistent polarized aug-cc-pVDZ basis set[15] was employed for all other atoms in these calculations. We determined the interaction energy between Trp44 and the metal ion bound to H36, M47, and M49 to be on the order of ∼14 kcal/mol (Table SI.1). We then estimated the contribution of the W44−(H36·M47·M49) interaction energy to the above energy by calculating the interaction energy between Trp44 and the other metal binding residues in the absence of the metal ion at the same geometry. While this method contains a certain amount of approximation, it yields an estimate for the "apo interaction energy" that is close to the interaction energy calculated from the 1ZEQ crystal structure geometry (−5.43 kcal/mol). From these calculations, we found that the $Cu^+/Ag^+$−W44 interactions afford a stabilization of >10 kcal/mol to the metal ion complex. A comparison of various functionals within the framework of density functional theory (DFT) paired with the aug-cc-pVDZ basis set found the M06-L,[16] M06-2X,[17] and wB97XD[18] functionals to be most suitable for studying such an interaction (Table SI.2). In addition to calculating these interaction energies, we performed a natural bond orbital analysis[19] to characterize the $Cu^+/Ag^+$ interaction with the C$\varepsilon$3 and C$\zeta$3 carbon atoms of Trp44 at the MP2 level of theory using the LANL2DZ pseudopotential-based basis set for $Ag^+$ and the aug-cc-pVDZ basis set for all other atoms. We found that $Cu^+$ and $Ag^+$ ions interact specifically with both Trp44 atoms (Table SI.3). As expected, these bond orders are lower than those of the $Cu^+/Ag^+$−S(Met47) bonds, indicating a relatively longer and weaker interaction. These low bond orders explain the marginal improvements seen by Xue et al.[7] and Loftin et al.[8] upon inclusion of a C/N/O scatterer in their models to fit EXAFS measurements.

To study the metal ion interactions in the W44M mutant, we investigated its $Cu^+$ binding environment by performing a series of increasingly complex DFT−QM/MM[20] calculations employing the M06-L functional. The final geometry optimization was performed using the LACV3P+* [11]basis set. Such methodologies provide powerful tools for elucidating protein function.[21−23] In these calculations, the W44M mutation was performed on wild-type (WT) CusF, and $Cu^+$ was allowed to decide its coordination in the solvated protein via energy minimization. Similar to the results of the NMR experiments performed by Loftin et al.,[9] we found that the W44M mutation does not change the protein structure (Figures SI.4 and SI.5). Our calculations showed that $Cu^+$ is bound to the His36, Met44, Met47, and Met49 residues in a distorted tetrahedral arrangement, as shown in Figure 3. In agreement with the EXAFS data, we found the bonds to $Cu^+$ to be longer than the corresponding bonds in WT CusF.[9] Interestingly, the $Cu^+$−S(M44) bond is shorter than the other $Cu^+$−S bonds to M47 and M49. The calculated bond lengths and bond angles are listed in Tables SI.4 and SI.5. The interaction energy between the bonded $Cu^+$ ion and Met44 in this binding motif was found to be −20.5 kcal/mol, with the $Cu^+$−Met44 interaction accounting for a stabilization energy of −20.7 kcal/mol (Table SI.1). The higher interaction energy and almost 2-fold greater stabilization energy observed for the W44M mutant are consistent with the higher binding affinity for $Cu^+$ in this mutant form.[7,9] While these calculations provide new insights about the binding environment of $Cu^+$ in W44M CusF, they are hindered


dx.doi.org/10.1021/ja208662z |J. Am. Chem. Soc. 2011, 133, 19330–19333

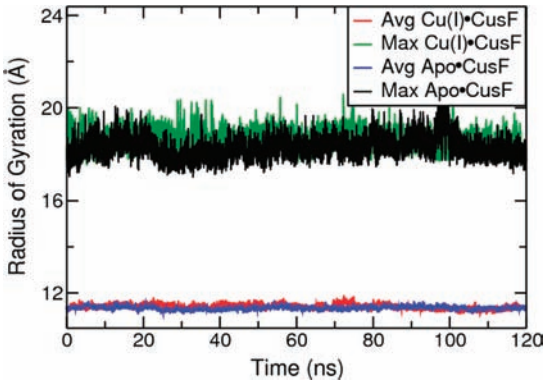


**Figure 4.** Average and maximum radii of gyration from simulations of apo and $Cu^+$-bound CusF.

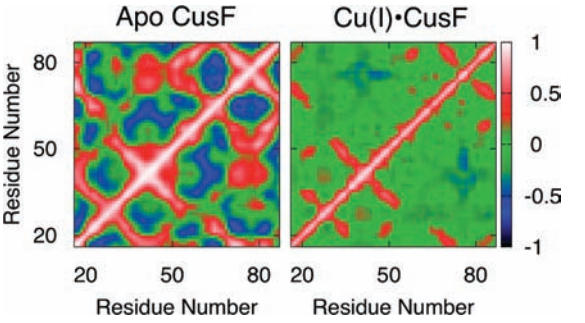


**Figure 5.** Cross-correlation plots for apo CusF and $Cu^+ \cdot$CusF.

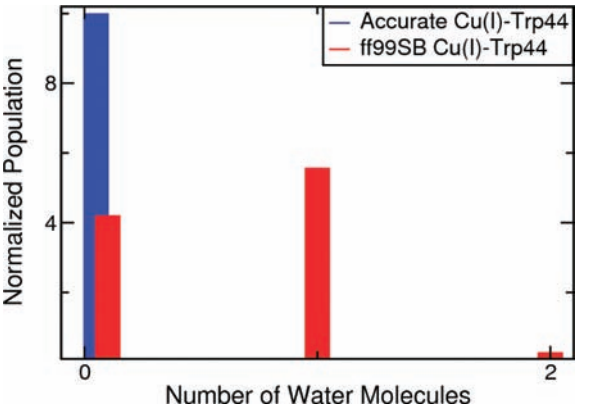


**Figure 6.** Distribution of water molecules in the first solvation shell of $Cu^+$ in simulations with a refined $Cu^+$—W44 interaction energy and the standard (weak) $Cu^+$—W44 interaction energy.

by an inherent lack of conformational sampling that may have introduced errors.

We analyzed changes in the protein's mobility and structure over 360 ns of all-atom MD simulations of the apo and $Cu^+$-bound forms of WT CusF in explicit solvent. We developed specific force-field parameters to treat $Cu^+$ as a bound ion in simulations of holo CusF. In addition, we modified the Lennard-Jones parameters on W44 to accurately portray the stronger $Cu^+$—W44 interaction obtained from our ab initio calculations. All of the parameters used in the study are included in the SI. A stable protein backbone root-mean-square deviation was observed over the course of our simulations of apo and $Cu^+$-bound CusF. The protein maintained its secondary structure, and no large-scale motions were detected in these simulations. The calculated average and maximum radii of gyration for the protein over the course of these simulations of apo CusF and $Cu^+ \cdot$CusF were similar (Figure 4), suggesting that $Cu^+$ binding does not alter the volume and size of the protein. Figure SI.6 depicts the calculated root mean square fluctuations of the C$\alpha$ backbone carbon atoms for the apo and $Cu^+$-bound states of the protein. The first eight residues in apo CusF remain very mobile. We observed a reduced mobility in most protein residues upon $Cu^+$ binding, in close agreement with the results of NMR experiments.[9] The $Cu^+$ binding residues are less mobile than their neighboring residues in apo CusF and become more rigid on metal ion binding. Trp44 does not actively search for the metal ion in the apo state and is preorganized to form a cation—$\pi$ interaction with the metal ion (Figures SI.6—SI.8). We found that the loop region defined by residues 72—80 moved significantly in our simulation of the apo allosteric form and did not become more rigid as a result of metal ion binding.

We further examined the impact of metal ion binding on protein residue motions by calculating the cross-correlation matrices for all backbone C$\alpha$ carbon atoms for the apo and $Cu^+$-bound states of the protein. These matrices map the correlation between the movements of various residues to values ranging from +1 for perfect correlation (i.e., movement in the same direction) to −1 for anticorrelation (i.e., movement in opposite directions). The apo state of the protein is characterized by a number of residues involved in correlated and anticorrelated motions (Figure 5). The metal binding residues move in a correlated manner in this allosteric form. We found that $Cu^+$ binding largely quenches the motions in the protein and causes some previously correlated residues to become anticorrelated and vice versa. The mobile loop region described by residues 40—43 and lying adjacent to the metal binding site now moves in an anticorrelated manner with the mobile loop formed by residues 72—80 and in a correlated manner with the loop formed by residues 26—30.

We investigated the function of Trp44 in the chaperone activity of CusF using QM/MM (M06-2X/LACVP*) calculations[11] and MD simulations. We calculated the energetic penalty to "swing" Trp44 away from $Cu^+$ along the $Cu^+$—C$\beta$—C$\gamma$—C$\delta$1 dihedral coordinate using QM/MM calculations (Figure SI.7). A scan along the dihedral coordinate at the crystal structure geometry of $Cu^+$-bound CusF revealed a significant energetic penalty associated with swinging of Trp44, preventing it from moving away from the metal ion. In addition, we found Trp44 to be locked in its position in our simulations of the apo and holo states of the protein. The C—C$\alpha$—C$\beta$—C$\gamma$ dihedral angle of Trp44 remained steady over the course of our simulation of apo CusF (Figure SI.8), suggesting that the metal binding site is preorganized for the cation—$\pi$ interaction between the metal ion and the Trp44 residue. We also examined the protective role of Trp44 in shielding the monovalent metal ion from oxidation by water molecules by performing an additional simulation of holo CusF with a weaker $Cu^+$—W44 interaction using standard ff99SB[24] Lennard-Jones parameters on W44. Upon comparing our two simulations of holo CusF, we observed no water molecules in the first solvation shell of the metal ion in our simulation with the correct $Cu^+$—W44 interaction energy, while water molecules were present near $Cu^+$ in over 60% of the snapshots from our simulation with a weaker $Cu^+$—W44 interaction energy (Figure 6). These results in conjunction with the low mobility of Trp44 demonstrate that the strong cation—$\pi$ interaction and the

hydrophobic nature of Trp44 successfully shield the $Cu^+$ ion from water molecules.

Our simulations highlight the role of protein motions in the chaperone function of CusF. CusF and CusB form a transient complex only when one of them is in the metal-bound state.[6,19] A recent chemical cross-linking and mass spectrometry study of CusF binding to CusB by Mealman et al.[25] suggests that residues 31−50 and 51−63 of CusF actively participate in interactions with CusB. These interactions are centered at the Lys31 and Lys58 residues. We obtained further support for these findings in our simulations. Lys31 and Lys58 remained relatively rigid in simulations of apo and $Cu^+$-bound CusF. Our simulations also found that residues in the CusF−CusB interaction regions become less mobile in the metal-bound state. In contrast, other parts of the protein not associated with CusB binding remain mobile in the $Cu^+$-bound states as well. These changes in protein residue mobility are accompanied by changes in the correlated motions as well. Our simulations strongly suggest that metal ion binding alters the internal motions in critical regions of the protein. These changes in the protein's conformational motions play an essential role in allowing CusF to form a transient complex with CusB and transfer $Cu^+/Ag^+$ to the cation efflux pump.

In this study, we used multiple computational approaches to provide detailed insights into the function and nature of the cation−$\pi$ interaction at the metal binding site of the periplasmic protein CusF. We quantified the $Cu^+/Ag^+$−W44 cation−$\pi$ interaction using high-level ab initio calculations and found a number of DFT functionals that accurately predict the energetics of the interaction. The calculated covalencies of the $Cu^+/Ag^+$ bonds to the C$\varepsilon$3 and C$\zeta$3 carbon atoms of W44 indicate that they are of a weak and long-range nature. We have proposed a distorted tetrahedral coordination geometry for $Cu^+$ in the W44M mutant and found the $Cu^+$−M44 interaction to be stronger than the cation−$\pi$ interaction in WT CusF. Our calculations show that Trp44 remains preorganized for metal ion binding and that the cation−$\pi$ interaction helps protect $Cu^+/Ag^+$ from oxidation in the periplasm. Our simulations suggest that no large conformational changes take place and that the protein maintains its structure in both allosteric forms on the time scale of hundreds of nanoseconds. We have found that $Cu^+$ binding quenches the internal dynamics of the protein. This was especially noticeable in residues that participate in the metal-ion-dependent interaction with the transmembrane periplasmic protein CusB. These results as a whole show that the $Cu^+/Ag^+$−W44 cation−$\pi$ interaction at the metal recognition site in WT CusF maintains a delicate balance between protecting $Cu^+$ from oxidation by water molecules and allowing the metal ion to be transferred to the tripartite cation efflux pump.

## ■ ASSOCIATED CONTENT

**Supporting Information.** Input files and information about all our calculations, figures, structures, force-field parameter files, the W44M protein structure, and complete refs 10 and 12. This material is available free of charge via the Internet at http://pubs.acs.org.

## ■ AUTHOR INFORMATION

**Corresponding Author**
merz@qtp.ufl.edu

## ■ ACKNOWLEDGMENT

We thank Benjamin P. Roberts, Sarah Gordon, and Naoya Asada for helpful discussions. We thank Thomas O'Halloran for directing our attention towards the W44M mutant. We gratefully acknowledge the National Institutes of Health (GM044974 and GM066859) for funding this project and the high-performance computing group at the University of Florida for their support.

## ■ REFERENCES

(1) Ma, Z.; Jacobsen, F. E.; Giedroc, D. P. *Chem. Rev.* **2009**, *109*, 4644.
(2) Munson, G. P.; Lam, D. L.; Outten, F. W.; O'Halloran, T. V. *J. Bacteriol.* **2000**, *182*, 5864.
(3) Franke, S.; Grass, G.; Rensing, C.; Nies, D. H. *J. Bacteriol.* **2003**, *185*, 3804.
(4) Su, C.-C.; Long, F.; Zimmermann, M. T.; Rajashankar, K. R.; Jernigan, R. L.; Yu, E. W. *Nature* **2011**, *470*, 558.
(5) Loftin, I. R.; Franke, S.; Roberts, S. A.; Weichsel, A.; Heroux, A.; Montfort, W. R.; Rensing, C.; McEvoy, M. M. *Biochemistry* **2005**, *44*, 10533.
(6) Kim, E.-H.; Rensing, C.; McEvoy, M. M. *Nat.Prod. Rep.* **2010**, *27*, 711.
(7) Xue, Y.; Davis, A. V.; Balakrishnan, G.; Stasser, J. P.; Staehlin, B. M.; Focia, P.; Spiro, T. G.; Penner-Hahn, J. E.; O'Halloran, T. V. *Nat. Chem. Biol.* **2008**, *4*, 107.
(8) Loftin, I. R.; Franke, S.; Blackburn, N. J.; McEvoy, M. M. *Protein Sci.* **2007**, *16*, 2287.
(9) Loftin, I. R.; Blackburn, N. J.; McEvoy, M. M. *J. Biol. Inorg. Chem.* **2009**, *14*, 905.
(10) Frisch, M. J.; et al. *Gaussian 09*, revision A.01; Gaussian, Inc.: Wallingford, CT, 2009.
(11) *Qsite*, version 5.7; Schrödinger, Inc.: New York, 2011.
(12) Case, D. A.; et al. *Amber 11*; University of California: San Francisco, 2010.
(13) Humphrey, W.; Dalke, A.; Schulten, K. *J. Mol. Graphics* **1996**, *14*, 33.
(14) Hay, P. J.; Wadt, W. R. *J. Chem. Phys.* **1985**, *82*, 299.
(15) Woon, D. E.; Dunning, T. H. *J. Chem. Phys.* **1993**, *98*, 1358.
(16) Zhao, Y.; Truhlar, D. G. *J. Chem. Phys.* **2006**, *125*, No. 194101.
(17) Zhao, Y.; Truhlar, D. G. *Theor. Chem. Acc.* **2008**, *120*, 215.
(18) Chai, J. D.; Head-Gordon, M. *Phys. Chem. Chem. Phys.* **2008**, *10*, 6615.
(19) Foster, J. P.; Weinhold, F. *J. Am. Chem. Soc.* **1980**, *102*, 7211.
(20) Warshel, A. *Computer Modeling of Chemical Reactions in Enzymes and Solutions*; Wiley: New York, 1991.
(21) Chakravorty, D. K.; Soudackov, A. V.; Hammes-Schiffer, S. *Biochemistry* **2009**, *48*, 10608.
(22) Hwang, J. K.; Warshel, A. *J. Am. Chem. Soc.* **1996**, *118*, 11745.
(23) Chakravorty, D. K.; Hammes-Schiffer, S. *J. Am. Chem. Soc.* **2010**, *132*, 7549.
(24) Hornak, V.; Abel, R.; Okur, A.; Strockbine, B.; Roitberg, A.; Simmerling, C. *Proteins* **2006**, *65*, 712.
(25) Mealman, T. D.; Bagai, I.; Singh, P.; Goodlett, D. R.; Rensing, C.; Zhou, H.; Wysocki, V. H.; McEvoy, M. M. *Biochemistry* **2011**, *50*, 2559.